Live and Let Die – A Systems Biology View on Cell Death

Thomas Eissing [a,*], Madalena Chaves [b], Frank Allgöwer [c]

[a] *Bayer Technology Services GmbH, PT-AS Systems Biology, Building 41, 51368 Leverkusen, Germany*

[b] *Institut National de Recherche en Informatique et Automatique, 2004 Route des Lucioles, BP93, 06902 Sophia-Antipolis, France*

[c] *Institute for Systems Theory and Automatic Control, University of Stuttgart, Pfaffenwaldring 9, 70550 Stuttgart, Germany*

Abstract

This contribution provides an overview of our work on modelling biological processes focussing on the example of programmed cell death, also called apoptosis. Apoptosis is a molecular programme present in all cells of multi-cellular organisms. It is crucial during development and for cell homoeostasis in the adult. Misregulation is implicated in severe diseases. We review an ordinary differential equation model describing core processes of apoptosis signalling and the idea of viewing the life and death decision as a bistable system. Then, we show how small differences in model parameters can give rise to observed population heterogeneities. Employing a new conceptional modelling framework, we further show how a single model can describe a population and how stable steady states then translate into invariant sets employing a local notion of stability.

Key words: systems biology, apoptosis, bistability, invariant sets

1 Introduction

Biology is a thriving science where exciting new discoveries are made almost on a daily basis. Thereby, biology has always been in close touch to other

* Corresponding author.
Email addresses: thomas.eissing@bayertechnology.com (Thomas Eissing), madalena.chaves@sophia.inria.fr (Madalena Chaves), allgower@ist.uni-stuttgart.de (Frank Allgöwer).

scientific disciplines which strongly contributed to its development. Quantitative reasoning based on mathematical considerations had strong and driving influences on biology (Wingreen and Botstein, 2006). On the other hand, with the emergence of molecular biology many exciting questions were raised and answered that did not require mathematical models to allow a qualitative understanding of many principle aspects that make up life. However, by now the wealth of information about molecular players and their interactions is becoming overwhelming and cannot be understood by merely drawing diagrams of the interacting components of a system. The human genome project does not mark the completion but the beginning of the next level of understanding. Mathematical biology, metabolic engineering and chemical engineering approaches towards the cell or an organism, for a long time regarded as peripheral sciences to biology, are emerging as the "post-(gen)omic" frontiers. Whereas the "-omic" technologies produce large amounts of data, systems biology is promising to integrate the wealth of information.

Thereby, systems biology can also be viewed as chemical engineering of the cell or the organism. As in chemical engineering processes, quantitative and dynamic modelling approaches describing aspects of, or on the long term, even the whole living cell or organisms, will become essential to organize and understand (biological) complexity. The analysis of these models will allow to more rapidly test biological hypothesis and provide insight not easily accessible by classical experimentation. However, a cell is a crowded environment where many thousand compounds and reactions happen simultaneously on a picolitre scale. Further, the involved systems are complex and usually involve nonlinear interactions (Kitano, 2002). Therefore, precise experimental data and advanced computational methods will be important requirements for sharp and useful dynamical models.

In this contribution we would like to overview selected aspects around our work to better understand apoptosis signalling using mathematical models. We will also introduce a novel modelling concept based on which we generalize the idea of bistable systems, to systems possessing two invariant sets.

2 Apoptosis biology

Apoptosis, also called programmed cell death, is a very important biological process that can eliminate selected cells for the benefit of the organisms as a whole. It is crucial during development and for cellular homoeostasis balancing cellular reproduction. In the adult human, approximately 10 billion cells die every day to balance those reproduced during mitosis (Heemels et al., 2000). Too little apoptosis and uncontrolled reproduction are hallmarks of cancer, whereas too much apoptosis is implicated in neurodegenerative diseases such

as Alzheimer (Danial and Korsmeyer, 2004; Hanahan and Weinberg, 2000).

As outlined in Fig. 1, apoptosis can be triggered externally, e.g. by certain cytokines binding to so-called death receptors, or internally, e.g. in response to DNA damage (Danial and Korsmeyer, 2004; Hanahan and Weinberg, 2000). Proteases, i.e. proteins able to cleave other proteins, named caspases are central in apoptosis signal transduction. Caspases are produced in an inactive pro-form and become activated through proteolytic cleavage. Initiator caspases sense apoptotic stimuli and propagate the signal to executioner caspases. These cleave many targets within the cell leading to its destruction and removal. For example, an inhibitor of the Caspase Activated DNase (ICAD) is cleaved liberating the DNase CAD to fragment nuclear DNA. Internally triggered apoptosis proceeds via mitochondrial cytochrome c release leading to the activation of the initiator caspase 9. Caspase 9 then activates executioner caspases, most prominently caspase 3 (C3). Externally triggered apoptosis is initiated by the binding of so-called death ligands such as Tumor Necrosis Factor (TNF) to their respective receptors, followed by the activation of receptor associated initiator caspases 8 and 10 (C8). It then proceeds either also via the activation of the mitochondrial pathway (type II) or by direct activation of caspase 3 (type I) (Scaffidi et al., 1998).

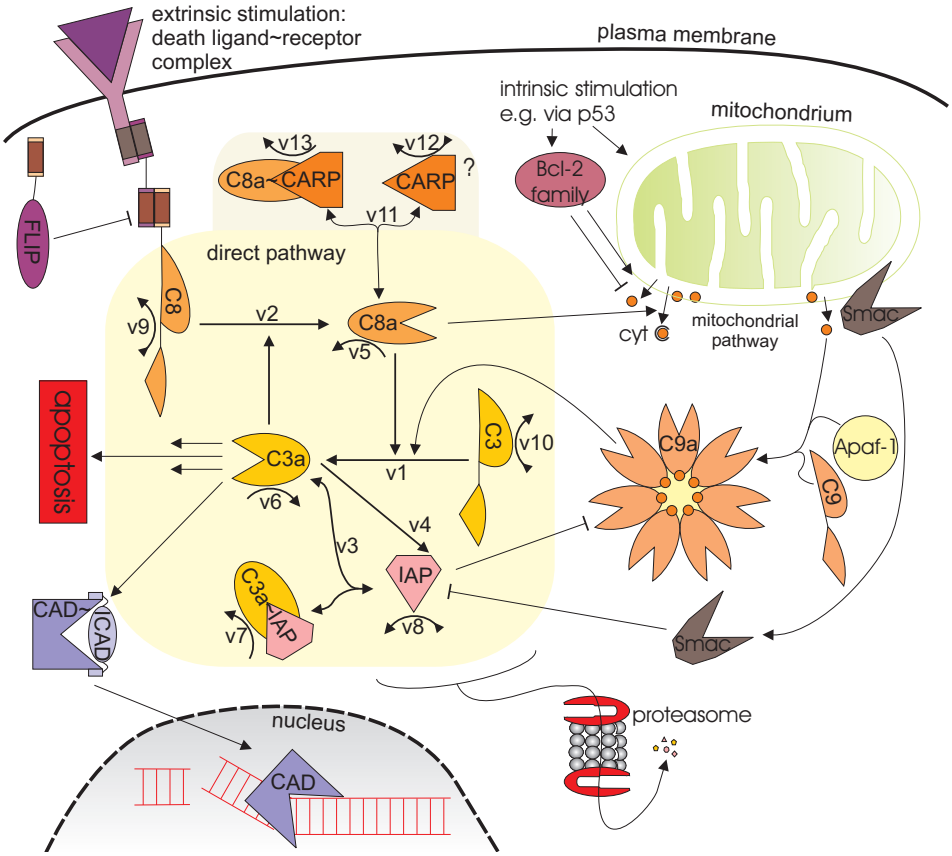

Fig. 1. Apoptosis signalling pathways.

These steps are regulated at different levels, e.g. Bcl-2 family member proteins regulate the mitochondrial cytochrome c release, or Inhibitor of Apoptosis Protein (IAP) family members inhibit activated caspases 3 and 9. In addition, positive feedback loops have been established yielding a complex reaction system (Sohn et al., 2005; Stennicke and Salvesen, 1999).

3 A model for the direct pathway of apoptosis

Graphical models as depicted in Fig. 1 are very useful to overview key processes of apoptosis signalling. However, these cannot (easily) capture important temporal and quantitative information. Therefore a mathematical model formulation is desirable.

Apoptosis involves the irreversible decision of whether a cell continues to live or dies. We translated this into the mathematical requirement for two stable steady states in a differential equation based model (Eissing et al., 2004). Experimental evidence suggest that this bistable behaviour is manifested in the caspase cascade. The activated upstream initiator caspase 8 is produced at the receptor level and can be considered as an input, while the activation of the downstream executioner caspase 3 is associated with apoptosis and can be considered as an output. Thereby, a low amount of C3a corresponds to "life" whereas a high amount corresponds to "programmed cell death" (Eissing, 2007). Also, on the single cell level the majority of caspase 3 is activated within minutes (Rehm et al., 2002, 2006). Accordingly, mathematical models of both the direct and the mitochondrial pathway of apoptosis have recently been evaluated for bistability (Eissing et al., 2004; Bagci et al., 2006; Legewie et al., 2006; Eissing et al., 2007a,b).

Based on extensive literature studies, we established a mathematical model of the core reactions of the direct pathway of apoptosis (including the reaction rates $v_1 - v_{10}$ indicated in Fig. 1 and detailed in Fig. 2). However, this basic model exhibited bistable behaviour only for parameter values orders of magnitudes away from those obtained from literature. Therefore, we considered an extended model (additionally including the reaction rates $v_{11} - v_{13}$) which is now supported by new experimental findings (Eissing et al., 2004; McDonald and El-Deiry, 2004). The bistable behaviour of the model is illustrated in Fig. 3a where we show the time evolution of C3a for different initial concentrations of C8a. As can be seen, for small input concentrations hardly any caspase 3 is activated, while for larger inputs almost all caspase 3 is activated within a very short time interval after a certain lag phase whose length is inversely related to the input strength. In comparison to this behaviour, Fig. 3b illustrates how a population of 20,000 cells, where each parameter of each cell was randomly chosen between 90 and 110 % of its original value, can yield a

As indicated in Fig. 1, we consider the following rates:

$$
\begin{aligned}
v_1 &= k_1 \cdot [C8a] \cdot [C3] \\
v_2 &= k_2 \cdot [C3a] \cdot [C8] \\
v_3 &= k_3 \cdot [C3a] \cdot [IAP] \\
&\quad - k_{-3}[C3aIAP] \\
v_4 &= k_4 \cdot [C3a] \cdot [IAP] \\
v_5 &= k_5 \cdot [C8a] \\
v_6 &= k_6 \cdot [C3a] \\
v_7 &= k_7 \cdot [C3aIAP] \\
v_8 &= k_8 \cdot [IAP] - k_{-8} \\
v_9 &= k_9 \cdot [C8] - k_{-9} \\
v_{10} &= k_{10} \cdot [C3] - k_{-10} \\
v_{11} &= k_{11} \cdot [C8a] \cdot [CARP] \\
&\quad - k_{-11} \cdot [C8aCARP] \\
v_{12} &= k_{12} \cdot [CARP] - k_{-12} \\
v_{13} &= k_{13} \cdot [C8aCARP].
\end{aligned}
\tag{1}
$$

The rate constants are given in the table to the right. Zero-order reaction constants are in $[molecules \cdot cell^{-1} \cdot min^{-1}]$, first-order reaction constants are in $[min^{-1}]$, and second-order reactions constants in $[molecules^{-1} \cdot cell \cdot min^{-1}]$. Further details and explanations can be found in Eissing et al. (2004).

Balancing (1) yields:

$$
\begin{aligned}
[\dot{C8}] &= -v_2 - v_9 \\
[\dot{C8a}] &= v_2 - v_5 - v_{11} \\
[\dot{C3}] &= -v_1 - v_{10} \\
[\dot{C3a}] &= v_1 - v_3 - v_6 \\
[\dot{IAP}] &= -v_3 - v_4 - v_8 \\
[C3a\dot{\sim}IAP] &= v_3 - v_7 \\
[\dot{CARP}] &= -v_{11} - v_{12} \\
[C8a\dot{\sim}CARP] &= v_{11} - v_{13},
\end{aligned}
\tag{2}
$$

with standard parameter values:

k_1	$5.8 \cdot 10^{-5}$	k_{11}	$5 \cdot 10^{-4}$
k_2	$1 \cdot 10^{-5}$	k_{12}	$1 \cdot 10^{-3}$
k_3	$5 \cdot 10^{-4}$	k_{13}	$1.16 \cdot 10^{-2}$
k_4	$3 \cdot 10^{-4}$	k_{-3}	0.21
k_5	$5.8 \cdot 10^{-3}$	k_{-8}	464
k_6	$5.8 \cdot 10^{-3}$	k_{-9}	507
k_7	$1.73 \cdot 10^{-2}$	k_{-10}	81.9
k_8	$1.16 \cdot 10^{-2}$	k_{-11}	0.21
k_9	$3.9 \cdot 10^{-3}$	k_{-12}	540
k_{10}	$3.9 \cdot 10^{-3}$		

Fig. 2. Model for the direct pathway of receptor induced apoptosis (Eissing et al., 2004).

completely different picture on the population level. Whereas the single cells show a rapid caspase 3 activation, the caspase 3 activity increases much slower on the population level. While the steady states are independent of the input strength in the deterministic model, the timing is different for different inputs resulting in an averaging on the population level. These qualitative differences reflect observed differences in single cell and population experiments, and are likely important for physiological function.

Thus, while a single cell has its own steady states and can respond very quickly, a population includes different cells of the same type with slightly different steady states and kinetics, so the response of the population as a whole can be graded rather than switch-like (Rehm et al., 2002; Tyas et al., 2000).

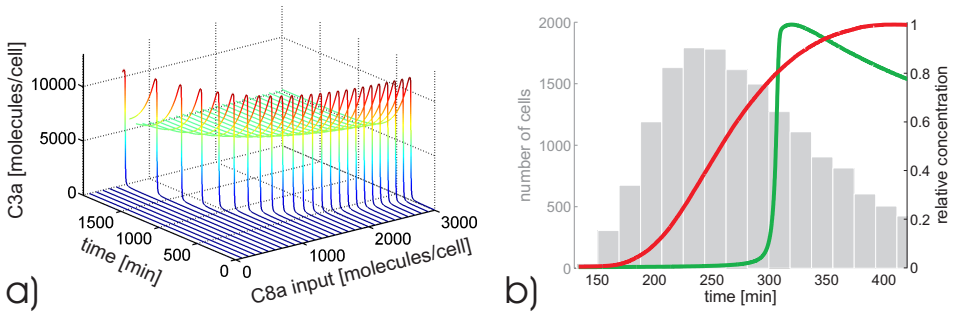

Fig. 3. a) Bistable behaviour of a model for the direct pathway of apoptosis (Eissing et al., 2004). b) Population behaviour (red) and (nominal) single cell behaviour (green) as relative concentrations of C3a for C8a(t=0) = 3,000 molecules/cell. The light grey bars indicate how many cells in the relevant time frame exceed a threshold of 500 molecules/cell C3a. 20,000 cells were simulated, each with parameters randomly chosen between 90 and 110 % of its original value.

4 Population and single cell modelling

This apparent difference between cell population and single cell responses, as exemplified above, has been experimentally detected in other biological systems which also exhibit bistability (for example, the *lac* operon in *E. Coli*, Ozbudak et al., 2004, and the cell cycle oscillator in *Xenopus laevis*, Pomerening et al., 2003). These observations suggest that experiments involving a population of cells may reflect an "average" response over all cells and represent the fraction of cells which are in a given steady state, for each given stimulus concentration. In reality, each cell has its own "threshold point" where the system jumps from one steady state to the other. This threshold point typically varies from cell to cell and depends on activation/inhibition constants, degradation rates, and other parameters of the system. For families of cells of the same type, these parameters may be expected to vary within a reasonably "small" region of the parameter space. Thus, cells in the same type exhibit similar qualitative behaviour, although within a certain variability margin.

4.1 0-Invariant sets and bistability

In deterministic continuous models, each steady state is associated with a single fixed point in the state space. However, since individual cells typically have their own specific operating points, it can be expected that also the mathematical fixed points will vary from cell to cell. For a whole population of cells of a single type, one can imagine that the individual fixed points will be contained in a well defined bounded set, such as a cube in several dimensions. Thus, a system is bistable if there are two such cubes (and disjoint) in the

state space: each cube represents one of the two stable responses of the system.

We have developed a method which allows one family of cells to be described by one general (deterministic and continuous) mathematical formulation, which incorporates cell-to-cell variability (Chaves et al., 2008). The class of models we propose is defined by *activation* and *inhibition* functions which vary within "tubes" (see below). In this way, the same model is flexible to accommodate the characteristic parameter values describing all individual cells in a given group. Moreover, intervals for the parameters can be determined, to guarantee that the system exhibits bistability (or monostability). Disjoint sets representing each of the stable responses are also characterized in terms of the parameters. In analogy with the definition of a *stable fixed point*, and using the language of control theory, we expect each of the response sets to be *a 0-invariant set for the system*. In other words, in the absence of stimuli (or zero input), once the trajectories enter this set, they will remain inside the set for all times. If a trajectory is evolving inside a 0-invariant set, it can only leave that set if an appropriate stimulus can be applied. For example, suppose that the caspase cascade is operating with low levels of active caspase; then only a sufficiently strong stimulation (e.g., with TNF) can activate the cascade and lead to high caspase levels.

The class of models proposed here, couples free (linear) degradation rates and an overall production rate. The latter is a combination of activation and inhibition functions, as determined by the network structure. Let N be a strictly positive real number. A function $\nu : [0, \infty) \to [0, N]$ is an *activation function* if:

(i) ν is continuously differentiable;
(ii) $0 < x < \infty$ implies $\nu(x) > 0$ and $\nu(0) = 0$;
(iii) There exists a threshold value $0 < \phi < \infty$ and constants $\varepsilon, \Delta \in (0, 1)$ such that

$$x \in [0, \phi(1-\Delta)) \;\Rightarrow\; \nu(x) \in [0, \varepsilon N),$$
$$x \in (\phi(1+\Delta), \infty) \;\Rightarrow\; \nu(x) \in (N(1-\varepsilon), N].$$

An *inhibition function* is defined in a similar manner, and can also be seen as: $\mu(x) = N - \nu(x)$. Observe that sigmoidal and also saturation type functions (corresponding to Hill or Michaelis-Menten kinetics), can be written in the form of ν or μ functions, with appropriate ε and Δ values.

Define c_3 = [C3a], c_8 = [C8a], y = [IAP], and u = [TNF] or an appropriate stimulus. In this framework, a reduced model for the caspase cascade network can be written as

$$
\begin{aligned}
\dot{c}_3 &= -k_3 c_3 + \nu_1(c_8)\mu_1(y) \\
\dot{c}_8 &= -k_8 c_8 + \nu_2(c_3) + \nu_3(u) \\
\dot{y} &= -k_{\text{IAP}} y + \mu_2(c_3) + \nu_4(u).
\end{aligned} \tag{3}
$$

This reduced model is intended to capture the *qualitative* dynamics resulting from four central interactions: mutual activation between C3a and C8a (represented by functions ν_1 and ν_2), and mutual inhibition between C3a and IAP (represented by functions μ_1 and μ_2). Following the definition of activation functions, the maximal value of each ν_i is denoted N_i while the maximal value of each μ_i is denoted M_i. Thus, the equation for c_3 reflects simply its degradation ($-k_3 c_3$) and its overall production ($\nu_1(c_8)\mu_1(y)$) rates. Equations for c_8 and y are similarly written, but an additive term is added to account for the effect of stimulation ($\nu_{3,4}(\text{TNF})$).

In the absence of inputs ($u = 0$), the maximal overall production rates are $V_{c_3} = N_1 M_1$, $V_{c_8} = N_2$, and $V_{\text{IAP}} = M_2$. Because the functions ν_i and μ_i are all bounded, the following cube is a 0-invariant and global attractor for system (3):

$$
Q = \left[0, \frac{V_{c_3}}{k_3}\right] \times \left[0, \frac{V_{c_8}}{k_8}\right] \times \left[0, \frac{V_{\text{IAP}}}{k_{\text{IAP}}}\right].
$$

Indeed, all trajectories of the system will eventually evolve inside this set: note that $\nu_1(c_8)\mu_1(y) \geq N_1 M_1 = V_{c_3}$ for all c_8 and all y, and

$$
c_3 > \frac{V_{c_3}}{k_3} \;\text{ implies }\; \dot{c}_3 < -k_3 \frac{V_{c_3}}{k_3} + N_1 M_1 < -V_{c_3} + V_{c_3} = 0,
$$

implying that c_3 strictly decreases towards $\frac{V_{c_3}}{k_3}$, whenever it starts above this value. Similar arguments can be applied to the variables c_8 and y. From now on, we will assume that trajectories evolve in Q and call the quotients V_{c_3}/k_3, V_{c_8}/k_8, and $V_{\text{IAP}}/k_{\text{IAP}}$ the *maximal values* of c_3, c_8 and y, respectively.

For some values of the parameters, this cascade may indeed exhibit bistable behaviour, in the sense that two disjoint 0-invariant sets exist, representing apoptosis ($\mathcal{A}$) and cell survival ($\mathcal{L}$). For other values of the parameters, it is possible to show that only one 0-invariant set exists, either representing apoptosis ($\mathcal{A}_*$) or cell survival ($\mathcal{L}_*$). Regions of parameters on which system (3) is bistable or monostable are indicated in Table 1. For all cases in this Table, the constants ε and Δ must satisfy the following conditions:

$$
\varepsilon < \frac{1}{2} \quad \text{and} \quad \Delta < 1 - 2\varepsilon.
$$

For the region of parameters were system (3) is bistable, the two stable responses of the cascade caspase can be identified with the two 0-invariant sets:

$$\mathcal{A} = \left[(1-\varepsilon)^2 \frac{V_{c_3}}{k_3}, \frac{V_{c_3}}{k_3}\right] \times \left[(1-\varepsilon)\frac{V_{c_8}}{k_8}, \frac{V_{c_8}}{k_8}\right] \times \left[0, \varepsilon \frac{V_{\mathrm{IAP}}}{k_{\mathrm{IAP}}}\right]$$

corresponding to an apoptotic response, since the levels of both caspases remain above an $1-\varepsilon$ fraction (higher than 50%) of their maximal values, and

$$\mathcal{L} = \left[0, \varepsilon^2 \frac{V_{c_3}}{k_3}\right] \times \left[0, \varepsilon \frac{V_{c_8}}{k_8}\right] \times \left[(1-\varepsilon)\frac{V_{\mathrm{IAP}}}{k_{\mathrm{IAP}}}, \frac{V_{\mathrm{IAP}}}{k_{\mathrm{IAP}}}\right]$$

corresponding to a living cell response, because the caspases are below an ε fraction (lower than 50%) of their maximal value (Fig. 4).

To establish that a given set is 0-invariant in a given region of parameters, one intuitive method is to compute the vector field at the boundary of the set, and show that it points towards the interior of the set: in other words, this guarantees that once a trajectory enters the set, it cannot leave the set. In the Appendix, we use this method to show that both sets $\mathcal{A}$ and $\mathcal{L}$ are 0-invariant for the bistability region of parameters indicated in Table 1.

Table 1
Conditions for bistability or monostability of the caspase cascade. $\phi_{X \dashv Z}$ (resp., $\phi_{X \to Z}$) denotes the threshold constant for inhibition (resp., activation) of species Z by X. A "high" expression level indicates that species is above a $1-\varepsilon$ fraction (above 50%) of its maximal value. Conversely, a "low" level indicates that species is below an ε fraction (below 50%) of its maximal value.

Steady states	Parameter quotients	Interval	Expression levels
Bistability	$\frac{V_{\mathrm{IAP}}}{k_{\mathrm{IAP}}} \frac{1}{\phi_{\mathrm{IAP} \dashv c_3}}$	$\left(\frac{1+\Delta}{1-\varepsilon}, \frac{1-\Delta}{\varepsilon}\right)$	$\mathcal{A}$: high C3a, C8a; low IAP
($\mathcal{A}$, $\mathcal{L}$)	$\frac{V_{c_3}}{k_3} \frac{1}{\phi_{c_3 \to c_8}}$, $\frac{V_{c_3}}{k_3} \frac{1}{\phi_{c_3 \dashv \mathrm{IAP}}}$	$\left(\frac{1+\Delta}{(1-\varepsilon)^2}, \frac{1-\Delta}{\varepsilon^2}\right)$	$\mathcal{L}$: low C3a, C8a;
	$\frac{V_{c_8}}{k_8} \frac{1}{\phi_{c_8 \to c_3}}$	$\left(\frac{1+\Delta}{1-\varepsilon}, \frac{1-\Delta}{\varepsilon}\right)$	high IAP
Monostability	$\frac{V_{\mathrm{IAP}}}{k_{\mathrm{IAP}}} \frac{1}{\phi_{\mathrm{IAP} \dashv c_3}}$	$(0, 1-\Delta)$	
(case I, $\mathcal{A}_*$)	$\frac{V_{c_3}}{k_3} \frac{1}{\phi_{c_3 \to c_8}}$	$\left(\frac{1+\Delta}{(1-\varepsilon)^2}, \infty\right)$	high C3a, C8a
	$\frac{V_{c_8}}{k_8} \frac{1}{\phi_{c_8 \to c_3}}$	$\left(\frac{1+\Delta}{1-\varepsilon}, \infty\right)$	any IAP
Monostability	$\frac{V_{c_8}}{k_8} \frac{1}{\phi_{c_8 \to c_3}}$	$(0, 1-\Delta)$	low C3a
(case II, $\mathcal{L}_*$)			any C8a, IAP

Not surprisingly, Table 1 shows that the capacity for bistability depends on

an appropriate balance between the maximal value of a variable X and the threshold constants for the links which are influenced by X. Interestingly, a very weak inhibition of C3a by IAP (high $\phi_{\mathrm{IAP}\dashv c_3}$) is not sufficient to guarantee apoptosis and prevent a bistable response. Similarly, a strong activation of C3a by C8a (low $\phi_{c_8\to c_3}$) alone is also not sufficient to guarantee apoptosis. Rather, both conditions should be verified to guarantee an apoptotic response (monostability, case I). In addition, C3a and C8a should be able to maintain each other, through the positive feedback cycle C3a $\leftrightharpoons$ C8a. In contrast, low activation of C3a by C8a (high $\phi_{c_8\to c_3}$) is sufficient to rule out apoptosis (monostability, case II).

Inhibitors of caspase 8 activation, such as CARP, may also be added to this model. The effect of CARP can be modelled, for instance, by decreasing the maximal production rate $N_2 = V_{c_8}$. From Table 1, it is easy to see that a pronounced decrease in V_{c_8} will fail to satisfy the conditions for bistability. Very low V_{c_8} leads to the condition for monostability (II), as might be expected.

4.2 Classifying cells: healthy or malfunctioning

Besides the bistable response, also conditions for two distinct monostable scenarios (I and II) can be found. The 0-invariant sets identified for each of the two monostable scenarios are

$$\mathcal{A}_* = \left[(1-\varepsilon)^2\frac{V_{c_3}}{k_3}, \frac{V_{c_3}}{k_3}\right] \times \left[(1-\varepsilon)\frac{V_{c_8}}{k_8}, \frac{V_{c_8}}{k_8}\right] \times \left[0, \frac{V_{\mathrm{IAP}}}{k_{\mathrm{IAP}}}\right]$$

and

$$\mathcal{L}_* = \left[0, \varepsilon\frac{V_{c_3}}{k_3}\right] \times \left[0, \frac{V_{c_8}}{k_8}\right] \times \left[0, \frac{V_{\mathrm{IAP}}}{k_{\mathrm{IAP}}}\right].$$

In each region of parameters, the sets $\mathcal{A}_*$ or $\mathcal{L}_*$ are 0-invariant (using the same method of computing the vector field at the boundary of the sets, and showing that it points towards the interior of the set). Furthermore, each set is also globally attractive: when caspase stimulation ceases, the system naturally converges to $\mathcal{A}_*$ (in scenario I) or $\mathcal{L}_*$ (in scenario II). Therefore, both scenarios represent anomalous or malfunctioning cells. In scenario I, there will eventually be a high level of active caspase 3, always leading the cell to the apoptotic pathway. In contrast, in scenario II the system will be depleted of active caspase 3, and be unable to go to the apoptotic pathway. Our analysis suggests that it is more difficult to find a cell which always goes through the apoptosis pathway, than a cell which always fails to have an apoptotic response – for scenario I *three conditions* on the parameters need to be satisfied, while

for scenario II *only one condition* needs to be satisfied. Indeed, among other diseases, the relatively common cancerous cells can be classified into case II, while not many diseases are known to be caused by "completely apoptotic" cells.

In conclusion, by measuring the production rates, as well as degradation rates and activation/inhibition thresholds for a given network, one can then check which of the conditions (Table 1) are satisfied. Once the system is classified, it may be possible to construct an appropriate input, or induces changes in some of the parameters, to control/restore the system to a desired behaviour.

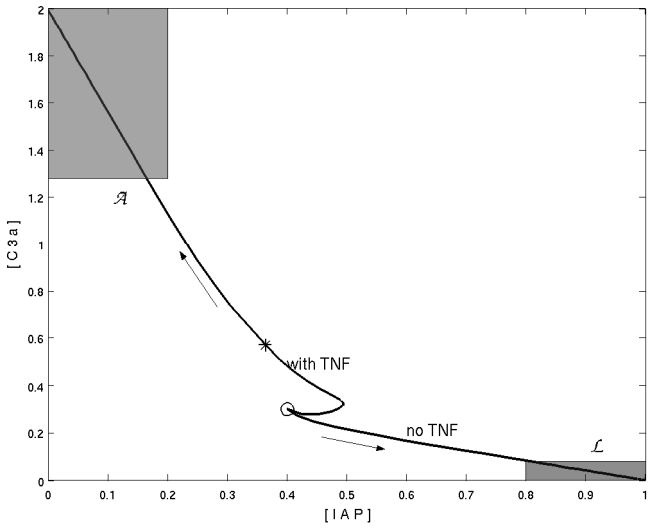

Fig. 4. The "apoptosis" ($\mathcal{A}$) and "living" ($\mathcal{L}$) 0-invariant sets, and two trajectories of system (3) projected into the (c_3, y)-plane. The two trajectories start from the same initial condition (o), $(c_3, c_8, y) = (0.3, 0.2, 0.4)$, for one realization of system (3). Parameters are as indicated in Section 4.3. One trajectory corresponds to no TNF stimulation (i.e., $\nu_3(\text{TNF}) = \nu_4(\text{TNF}) = 0$), and converges to the "living" set. The other trajectory corresponds to constant TNF stimulation with $\nu_3(\text{TNF}) = 1$ and $\nu_4(\text{TNF}) = 0.1$ and converges to the apoptosis set. Stimulation duration is 1.5 time units (total running time is 15 units). The symbol $*$ marks the state at the point when TNF was turned off.

4.3 TNF stimulation

So far, the behavior of the system, and its capacity for bistability, have been analysed in the case without stimulation. We will now briefly analyse the effect of, for example, TNF stimulation. Suppose that the system is in a state with low caspase levels, for instance point "o" in Fig. 4. Constant TNF stimulation during a sufficiently long interval increases the concentration of active

caspase 8. This is immediate by looking at the equation $\dot{c}_8 \geq -k_8 c_8 + \nu_3(\text{TNF})$ which implies that $c_8(t)$ increases faster than $\nu_3(\text{TNF})(1-e^{-k_8 t})/k_8$. Similarly, TNF stimulation also induces an increase in IAP concentration (via the NFκB pathway not further discussed in this contribution). However, C8a promotes and IAP opposes resistance to increasing the concentration of C3a. If the activation effect of C8a is stronger than the inhibition effect of IAP, then C3a concentration tends to increase. If the trajectory reaches $\mathcal{A}$ (or its basin of attraction), since $\mathcal{A}$ is a 0-invariant set for the system, TNF stimulation may now be "turned off" and the system continues to evolve in $\mathcal{A}$, thus enabling the cell to enter the apoptotic pathway.

This behaviour is illustrated in Fig. 4, with one realization of system (3). A set of parameters satisfying the bistability conditions, and appropriate activation and inhibition functions were chosen as follows: $\varepsilon = 0.2$, $\Delta = 0.48$, $k_3 = k_8 = k_{\text{IAP}} = 1$, $N_1 = 2$, $N_2 = M_1 = M_2 = 1$, $\phi_{c_8 \to c_3} = \phi_{\text{IAP} \dashv c_3} = 0.4$, and $\phi_{c_3 \to c_8} = \phi_{c_3 \dashv \text{IAP}} = 0.3$. The functions ν_i and μ_i $(i = 1, 2)$ are Hill functions with maximal amplitude, respectively, N_i and M_i, Hill exponent equal to 6, and threshold values $\phi_{\ldots}$ as indicated before. Since $u =$TNF is assumed constant, the terms $\nu_{3,4}(TNF)$ were simply set to 0 (no TNF stimulation) or $\nu_3(\text{TNF}) \equiv 1$, $\nu_4(\text{TNF}) \equiv 0.1$ for one time unit (with TNF stimulation).

5 Discussion and Conclusions

In this study we introduced the need for quantitative modelling approaches in biology by discussing the example of apoptosis signalling. We reviewed a bistable apoptosis model for the direct pathway of receptor induced apoptosis and illustrated how small parameter differences can explain different behaviours on the single cell and population level. While the activation of caspase 3, a key molecule in apoptosis, is slow on the population level, it is rapidly activated on the single cell level. The different timing in individual cells can also be explained, for example, by a distributed input (Eissing et al., 2004) or different protein concentrations. Extended analysis in the context of robustness, which appears to be an important property of many biological systems (Stelling et al., 2004), indicate that the cell has achieved a favourable robustness-performance trade-off, imposed by network structure and evolutionary constraints. On the one hand, inhibitors of apoptosis function as noise filters and reduce variability caused by the stochastic nature of reactions (Eissing et al., 2005). Further, qualitative properties such as bistability are comparably robust to parameter changes supporting proper decisions. On the other hand, quantitative aspects are comparably sensitive. This allows for variability in a population, as observed in experiments, and which is likely important for physiological function as recently indicated in immunological studies (Hawkins et al., 2007). Our analyses further indicated that the trade-off leads to fragili-

ties. For example, an up-regulation of IAPs, as observed in certain cancers, can not only desensitise cells to apoptotic stimuli, as also suggested by experimental studies, but can contribute to cancer aggressiveness and progression through additional mechanisms (Eissing, 2007).

We further introduced a new modelling framework, which describes reactions by generalized activation and inhibition functions. Bistable systems can then be characterized by possessing two disconnected invariant sets. This description nicely integrates differences between single cells into one model. Pathological cellular states can be identified and characterized by the presence of a single, globally attractive set. Two cases can be distinguished, one representing apoptosis resistant cells and one representing hypersensitive cells, both of which are known to exist.

The presented models can be extended to integrate alternative routes of apoptosis signalling as outlined in Fig. 1. Also, several additional signalling pathways are known that can fine-tune or even strongly influence the decision on whether a cell continues to life or dies (e.g. Janes et al. 2005, 2006). Certainly, much more work will be needed before a system-level understanding of apoptosis and, more generally, biology is achieved. Thereby, the involved scales in biology and the inherent complexity pose great challenges. However, the potential rewards are high – strong and lasting influences on biotechnology and a rationalization of medicine are to be expected. In biotechnology, for example, model based considerations are already maximizing product yields, and the first drug candidates whose targets were indicated by analysing mathematical models are under investigation.

Acknowledgements

The described work is supported by the Deutsche Forschungsgemeinschaft (DFG) and the Centre for Systems Biology Stuttgart funded by the state of Baden-Württemberg. The authors would like to thank the involved partners, especially Eric Bullinger and Peter Scheurich.

Appendix: Checking 0-invariance of sets $\mathcal{A}$ and $\mathcal{L}$

Consider the region of parameters defined in Table 1, under "Bistability". They can be written as:

$$(1.1)\quad \frac{V_{\text{IAP}}}{k_{\text{IAP}}}\frac{1}{\phi_{\text{IAP}\dashv c_3}} > \frac{1+\Delta}{1-\varepsilon}$$
$$(1.2)\quad \frac{V_{\text{IAP}}}{k_{\text{IAP}}}\frac{1}{\phi_{\text{IAP}\dashv c_3}} < \frac{1-\Delta}{\varepsilon}$$
$$(2.1)\quad \frac{V_{c_3}}{k_3}\frac{1}{\phi_{c_3\to c_8}}, \frac{V_{c_3}}{k_3}\frac{1}{\phi_{c_3\dashv \text{IAP}}} > \frac{1+\Delta}{(1-\varepsilon)^2}$$
$$(2.2)\quad \frac{V_{c_3}}{k_3}\frac{1}{\phi_{c_3\to c_8}}, \frac{V_{c_3}}{k_3}\frac{1}{\phi_{c_3\dashv \text{IAP}}} < \frac{1-\Delta}{\varepsilon^2}$$
$$(3.1)\quad \frac{V_{c_8}}{k_8}\frac{1}{\phi_{c_8\to c_3}} > \frac{1+\Delta}{1-\varepsilon}$$
$$(3.2)\quad \frac{V_{c_8}}{k_8}\frac{1}{\phi_{c_8\to c_3}} < \frac{1-\Delta}{\varepsilon}$$

Under these conditions, both $\mathcal{L}$ and $\mathcal{A}$ are 0-invariant sets. The arguments used for one set or the other are very similar. Thus, we will present only the 0-invariance for $\mathcal{A}$.

We will pick any point P at the boundary of $\mathcal{A}$ and show that the vector field points towards the interior of the set, whenever the parameter satisfy the given conditions. First, note that $\mathcal{A}$ is contained in the cube Q, which is also a (large) invariant set for the system. Note also that, at points of the form $(\frac{V_{c_3}}{k_3}, c_8, y)$, $(c_3, \frac{V_{c_8}}{k_8}, y)$ or $(c_3, c_8, 0)$, the boundary of $\mathcal{A}$ coincides with the boundary of Q. Thus, at these points, the vector field points towards the interior of Q and $\mathcal{A}$.

For points of the form

$$P_3 = \left(\frac{(1-\varepsilon)^2 V_{c_3}}{k_3}, c_8, y\right), \quad c_8, y \in \left[(1-\varepsilon)\frac{V_{c_8}}{k_8}, \frac{V_{c_8}}{k_8}\right] \times \left[0, \varepsilon\frac{V_{\text{IAP}}}{k_{\text{IAP}}}\right]$$

it follows from (1.2) and (3.1) that

$$y \le \varepsilon\frac{V_{\text{IAP}}}{k_{\text{IAP}}} < \varepsilon\frac{1-\Delta}{\varepsilon}\phi_{\text{IAP}\dashv c_3}$$
$$c_8 \ge (1-\varepsilon)\frac{V_{c_8}}{k_8} > (1-\varepsilon)\frac{1+\Delta}{1-\varepsilon}\phi_{c_8\to c_3}$$

which implies, using the definition of activation and inhibition functions,

$$y < (1-\Delta)\phi_{\text{IAP}\dashv c_3} \quad\Rightarrow\quad \mu_1(y) > (1-\varepsilon)M_1$$
$$c_8 > (1+\Delta)\phi_{c_8\to c_3} \quad\Rightarrow\quad \nu_1(c_8) > (1-\varepsilon)N_1.$$

Then, looking at the c_3 equation, and recalling that $V_{c_3} = N_1 M_1$:

$$\begin{aligned}\dot{c}_3 &> -k_3\frac{(1-\varepsilon)^2V_{c_3}}{k_3} + (1-\varepsilon)M_1(1-\varepsilon)N_1\\ &= -(1-\varepsilon)^2V_{c_3} + (1-\varepsilon)^2V_{c_3} = 0,\end{aligned}$$

which means that for points of the form P_3, c_3 will increase, i.e., the vector field points towards the interior of $\mathcal{A}$.

A similar argument can be used for points of the form

$$P_8 = \left(c_3, \frac{(1-\varepsilon)V_{c_8}}{k_8}, y\right), \quad c_3, y \in \left[(1-\varepsilon)^2\frac{V_{c_3}}{k_3}, \frac{V_{c_3}}{k_3}\right] \times \left[0, \varepsilon\frac{V_{\text{IAP}}}{k_{\text{IAP}}}\right].$$

It follows from (2.1) that

$$c_3 \geq (1-\varepsilon)^2\frac{V_{c_3}}{k_3} > (1-\varepsilon)^2\frac{1+\Delta}{(1-\varepsilon)^2}\phi_{c_3\to c_8},$$

which implies, using the definition of activation function,

$$c_3 > (1+\Delta)\phi_{c_3\to c_8} \quad \Rightarrow \quad \nu_2(c_3) > (1-\varepsilon)N_2.$$

Then, looking at the c_8 equation, and recalling that $V_{c_8} = N_2$:

$$\begin{aligned}\dot{c}_8 &> -k_8\frac{(1-\varepsilon)V_{c_8}}{k_8} + (1-\varepsilon)N_2\\ &= -(1-\varepsilon)V_{c_8} + (1-\varepsilon)V_{c_8} = 0,\end{aligned}$$

which means that for points of the form P_8, c_8 will increase, i.e., again the vector field points towards the interior of $\mathcal{A}$.

Finally, for points of the form

$$P_{\text{IAP}} = \left(c_3, c_8, \varepsilon\frac{V_{\text{IAP}}}{k_{\text{IAP}}}\right), \quad c_3, c_8 \in \left[(1-\varepsilon)^2\frac{V_{c_3}}{k_3}, \frac{V_{c_3}}{k_3}\right] \times \left[(1-\varepsilon)\frac{V_{c_8}}{k_8}, \frac{V_{c_8}}{k_8}\right].$$

it follows from (2.1) that

$$c_3 \geq (1-\varepsilon)^2\frac{V_{c_3}}{k_3} > (1-\varepsilon)^2\frac{1+\Delta}{(1-\varepsilon)^2}\phi_{c_3\vdash\text{IAP}},$$

which implies, using the definition of inhibition function,

$$c_3 > (1+\Delta)\phi_{c_3\vdash\text{IAP}} \quad \Rightarrow \quad \mu_2(c_3) < \varepsilon M_2.$$

Then, looking at the y equation, and recalling that $V_{\text{IAP}} = M_2$:

$$\begin{aligned}\dot{y} &> -k_{\text{IAP}}\varepsilon\frac{V_{\text{IAP}}}{k_{\text{IAP}}} + \varepsilon M_2 \\ &= -\varepsilon V_{\text{IAP}} + \varepsilon V_{\text{IAP}} = 0,\end{aligned}$$

which means that for points of the form P_{IAP}, y will increase, i.e., again the vector field points towards the interior of $\mathcal{A}$.

References

Bagci, E. Z., Vodovotz, Y., Billiar, T. R., Ermentrout, G. B., Bahar, I., 2006. Bistability in apoptosis: Roles of Bax, Bcl-2 and mitochondrial permeability transition pores. Biophys. J. 90, 1546–1559.

Chaves, M., Eissing, T., Allgöwer, F., 2008. Bistable biological systems: a characterization through local compact input-to-state stability. IEEE Transactions on Automatic Control 53 (1), 87–100.

Danial, N. N., Korsmeyer, S. J., 2004. Cell death: critical control points. Cell 116 (2), 205–219.

Eissing, T., 2007. A systems science view on cell death signalling. PhD thesis, University of Stuttgart & Fortschr.-Ber. VDI Reihe 8, Nr. 1137, VDI-Verlag Düsseldorf.

Eissing, T., Allgöwer, F., Bullinger, E., 2005. Robustness properties of apoptosis models with respect to parameter variations and stochastic influences. IEE Syst. Biol. 152 (4), 221–228.

Eissing, T., Conzelmann, H., Gilles, E. D., Allgöwer, F., Bullinger, E., Scheurich, P., 2004. Bistability analyses of a caspase activation model for receptor-induced apoptosis. J. Biol. Chem. 279 (35), 36892–36897.

Eissing, T., Waldherr, S., Allgöwer, F., Scheurich, P., Bullinger, E., 2007a. Response to Bistability in Apoptosis: Roles of Bax, Bcl-2, and Mitochondrial Permeability Transition Pores. Biophys. J. 92 (9), 3332–3334.

Eissing, T., Waldherr, S., Allgöwer, F., Scheurich, P., Bullinger, E., 2007b. Steady state and (bi-) stability evaluation of simple protease signalling networks. BioSystems 90 (3), 591–601.

Hanahan, D., Weinberg, R. A., 2000. The hallmarks of cancer. Cell 100 (1), 57–70.

Hawkins, E. D., Turner, M. L., Dowling, M. R., van Gend, C., Hodgkin, P. D., 2007. A model of immune regulation as a consequence of randomized lymphocyte division and death times. Proc. Natl. Acad. Sci. U. S. A. 104 (12), 5032–5037.

Heemels, M. T., Dhand, R., Allen, L., 2000. Apoptosis. Nature 407 (6805), 769.

Janes, K. A., Albeck, J. G., Gaudet, S., Sorger, P. K., Lauffenburger, D. A.,

Yaffe, M. B., 2005. A systems model of signaling identifies a molecular basis set for cytokine-induced apoptosis. Science 310 (5754), 1646–1653.

Janes, K. A., Gaudet, S., Albeck, J. G., Nielsen, U. B., Lauffenburger, D. A., Sorger, P. K., 2006. The response of human epithelial cells to TNF involves an inducible autocrine cascade. Cell 124 (6), 1225–1239.

Kitano, H., 2002. Systems biology: a brief overview. Science 295 (5560), 1662–1664.

Legewie, S., Blüthgen, N., Herzel, H., 2006. Mathematical Modeling Identifies Inhibitors of Apoptosis as Mediators of Positive Feedback and Bistability. PLoS Comput. Biol. 2 (9), e120.

McDonald, 3rd, E. R., El-Deiry, W. S., 2004. Suppression of caspase-8- and -10-associated RING proteins results in sensitization to death ligands and inhibition of tumor cell growth. Proc. Natl. Acad. Sci. U. S. A. 101 (16), 6170–6175.

Ozbudak, E. M., Thattai, M., Lim, H. N., Shraiman, B. I., Oudenaarden, A. V., 2004. Multistability in the lactose utilization network of Escherichia coli. Nature 427 (6976), 737–740.

Pomerening, J., Sontag, E., J.E. Ferrell, Jr., 2003. Building a cell cycle oscillator: hysteresis and bistability in the activation of Cdc2. Nat. Cell Biol. 5, 346–351.

Rehm, M., Dussmann, H., Janicke, R. U., Tavare, J. M., Kogel, D., Prehn, J. H., 2002. Single-cell fluorescence resonance energy transfer analysis demonstrates that caspase activation during apoptosis is a rapid process. J. Biol. Chem. 277 (27), 24506–24514.

Rehm, M., Huber, H. J., Dussmann, H., Prehn, J. H. M., 2006. Systems analysis of effector caspase activation and its control by X-linked inhibitor of apoptosis protein. EMBO J. 25 (18), 4338–4349.

Scaffidi, C., Fulda, S., Srinivasan, A., Friesen, C., Li, F., Tomaselli, K. J., Debatin, K. M., Krammer, P. H., Peter, M. E., 1998. Two CD95 (APO-1/Fas) signaling pathways. EMBO J. 17 (6), 1675–1687.

Sohn, D., Schulze-Osthoff, K., Jänicke, R. U., 2005. Caspase-8 can be activated by interchain proteolysis without receptor-triggered dimerization during drug-induced apoptosis. J. Biol. Chem. 280 (7), 5267–5273.

Stelling, J., Sauer, U., Szallasi, Z., Doyle, 3rd, F. J., Doyle, J., 2004. Robustness of cellular functions. Cell 118 (6), 675–685.

Stennicke, H. R., Salvesen, G. S., 1999. Catalytic properties of the caspases. Cell Death Differ. 6 (11), 1054–1059.

Tyas, L., Brophy, V. A., Pope, A., Rivett, A. J., Tavare, J. M., 2000. Rapid caspase-3 activation during apoptosis revealed using fluorescence-resonance energy transfer. EMBO Rep. 1 (3), 266–270.

Wingreen, N., Botstein, D., 2006. Back to the future: education for systems-level biologists. Nat. Rev. Mol. Cell Biol. 7 (11), 829–832.